Renewable Energy 62 (2014) 417–423

Contents lists available at ScienceDirect

Renewable Energy

journal homepage: www.elsevier.com/locate/renene

The impact of large-scale distributed generation on power grid and microgrids

Qian Ai*, Xiaohong Wang, Xing He

School of Electronic Information and Electrical Engineering, Shanghai Jiaotong University, Minhang District, Shanghai 200240, China

ARTICLE INFO

Article history:
Received 23 May 2012
Accepted 16 July 2013
Available online

Keywords:
Distributed generation (DG)
Microgrid
Improved continuous flow method

ABSTRACT

With the widespread application of distributed generation (DG), their utilization rate is increasingly higher and higher in the power system. This paper analyzes the static and transient impact of large-scale DGs integrated with the distribution network load models on the power grid. Studies of static voltage stability based on continuous power flow method have shown that a reasonable choice of DG's power grid position will help to improve the stability of the system. The transient simulation results show that these induction motors in the distribution network would make effect on the start-up and fault conditions, which may cause the instability of DGs and grid. The simulation results show that modeling of distributed generations and loads can help in-depth study of the microgrid stability and protection design.

1. Introduction

A large number of DGs connected with the power grid will make a certain effect on all aspects of power system operation. Voltage stability is also an important aspect which has become one of the important research topics in the smart grid development [1–4].

Researchers have used different methods to construct a variety of stability index to study the voltage stability problem [5–9]. Voltage stability analysis includes two parts: the static stability and dynamic stability. The indicators measuring static voltage security and stability are as follows: various types of sensitivity index, the Jacobi matrix singular index, the minimum modulus eigenvalue index, distance index between the multiple solutions of flow in the load space, threshold voltage index and margin index ΔP, ΔQ and ΔV [10]. Among them, the margin index with good linearity is widely used in power system stability analysis.

Dynamic stability analysis of distribution network with DGs should consider a large number of induction motor loads in the distribution network. The load model is critical to the study of dynamic stability on the power grid as well. In particular, the transient stability problem of the rotation type DGs must be taken into account after power grid commits fault. If the power system becomes unstable after a fault, not to remove the DGs will take a negative impact on it. For example, the induction generator would absorb a large amount of reactive power from the system so as to causing the system voltage to drop. Generally it requires removing the DGs if the power grid faults occur.

From a control theory point of view, the power system is a very high-order multivariable process, operating in a constantly changing environment. Because of the high dimensionality and complexity of the system, it is essential to simplify assumptions and to analyze specific problems using the equivalent system model with right detailed-degree. This requires a good grasp of the characteristics of the overall system as well as its individual elements [11].

Reference [12] uses Newton Raphson power flow method to estimate the power system stability limit, it can give reasonable results, but may also cause convergence problems, and this method is very time-consuming. So its application is limited. Some scholars use parameter sensitivity to estimate the voltage stability [13]. Reference [14] calculates the voltage collapse critical point by an improved zero-eigenvalue method. Based on artificial neural networks method, reference [15] assesses the voltage security after the complex power system fault. Based on the above literatures this paper has improved the continuation flow method.

In order to study the static stability influence of DG on the power grid, firstly, it analyzes the power flow models of DFIG, PV, and battery storage, and then taking IEEE 30-bus system as an example. This paper uses an improved continuous flow method to obtain voltage stability limit point of the power gird with or without DG respectively, and analyzes the influence of the DG on load margin. Then, it discusses the dynamic effects on the microgrid in the case of motor start-up and power grid fault.

* Corresponding author.
E-mail address: aiqian@sjtu.edu.cn (Q. Ai).

0960-1481/$ – see front matter © 2013 Elsevier Ltd. All rights reserved.
http://dx.doi.org/10.1016/j.renene.2013.07.032

2. Static voltage stability analysis of DG on the power grid

2.1. DG flow models

2.1.1. The power flow calculation model of the double-fed induction generator (DFIG)

The stator of DFIG is connected to the power grid, and its rotor provides the excitation current through bi-directional converter connected to the power grid. It realizes AC excitation of rotor side by controlling the converter to determine the frequency, amplitude and phase angle of rotor excitation current.

In this control mode, the running of wind turbines has four work zones: start-up zone, wind tracking zone, constant speed zone, and the constant power zone.

When stator voltage of DFIG is equal to the power grid voltage, the operation state of DFIG off the power grid with no-load and that of DFIG on the power grid with zero output power is the same, so its power grid control is a special case of the power decoupling control ($P = 0$, $Q = 0$). It can be processed as PQ node in the power flow calculation.

2.1.2. The power flow calculation model of solar power generation system

Under normal circumstances, the grid-connected PV systems only provide active energy to the power grid, namely convert the DC energy of the solar photovoltaic array to the AC energy with the same frequency and phase to feed to the power grid, ensuring that it has a high power factor. Therefore, in the power flow calculation solar power grid nodes can be processed as PQ nodes, or as PQ nodes with $Q = 0$ under the control of the MPPT [16–21]. During power flow calculation, the active power and current injected into the power grid of photovoltaic cells are constant values and the injected reactive power is as follows:

$$Q = \sqrt{I^2(e^2+f^2) - P^2} \tag{1}$$

where P is the constant active power of output, I is a constant current injected into the power grid, e and f are the real and imaginary parts of the voltage at the DG nodes respectively. Calculating the real and imaginary parts of voltage in each iteration and the injected reactive power according to Eqn. (1), and then in the next iteration it is converted to PQ node.

2.1.3. The power flow calculation model of battery power system

Control of the battery is basically the same as that of a solar power generation system, the output DC voltage is converted to AC voltage so as to connect to network. The difference is that the battery can be not only used as the power source of the power grid but also used as the load on the power grid. The equivalent circuit of fuel cell connected with power grid shown in Fig. 1.

In Fig. 1, U_{FC} is the output DC voltage of the fuel cell, R_{FC} is the equivalent resistance of the fuel cell, m is the modulation index of the inverter, ψ is the lead angle of the inverter, U_{ac} is inverter output AC voltage of the inverter, X_T is the equivalent impedance of the transformer, Us is the bus voltage of network, δ and θ are the phase angle of voltage, with the relationship of $\psi = \delta - \theta$.

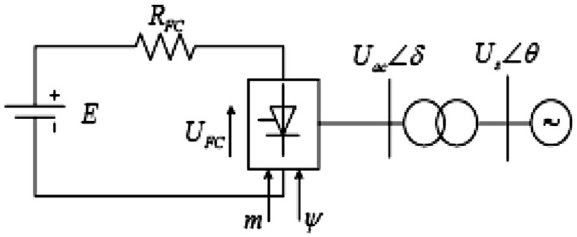

Fig. 1. Equivalent circuit of storage battery connected power grid.

Since $U_{ac} = mU_{Fc}$, combined with the equivalent circuit diagram of the fuel cell on the power grid, we can derive the following relation:

$$P = \frac{U_{ac}U_s}{X_T}\sin(\delta-\theta) = \frac{mU_{FC}U_s}{X_T}\sin(\psi) \tag{2}$$

$$Q = \frac{mU_{FC}U_s}{X_T}\cos(\psi) - \frac{U_s^2}{X_T} \tag{3}$$

The output active power of the fuel cell can be adjusted by controlling the parameter ψ, the output reactive power of batteries can be adjusted by controlling m, which is similar to the active power and reactive power regulation principle of conventional generator. So it is usually regarded as a PV node in the power flow calculation.

Given that Rated active power of the converter output is P_N, the minimum power factor is $\rho_{\min}$, and then the maximum capacity of the converter is:

$$S_{\max} = P_N/\rho^2 \tag{4}$$

Now the maximum reactive power of converter output corresponding to the active power P is:

$$Q_{\max} = \sqrt{S_{\max}^2 - P^2} \tag{5}$$

The fuel cell in the normal operating does not require absorbing reactive power from the power grid. It can be considered that the minimum reactive power is 0. If the reactive power of the battery node is exceeding the boundary, it can be processed as a PQ node, and reactive power injected is the upper or lower limit of the output reactive power.

2.1.4. The flow calculation model of the microturbine power generation system

The general working principle of microturbine is similar to the synchronous generator, with the speed control system and excitation system. Because the microturbine has a high rotational speed and the alternator has a very high frequency, its output is high frequency AC power [22]. It should supply load with the AC power which has stable output voltage and rated frequency by electronic converter.

So microturbine is processed as the PV node, similar to the approach of battery.

2.2. Static voltage stability analysis of power grid with DG

After the DG incorporating into distribution network, the radial structure of distribution network will become the multi-power structure, which may cause the system nodal voltage to change. The voltage of traditional radial distribution network under steady-state operation is gradually reduced along the direction of the power flow of the feeder. After DGs connecting with the grid, due to the reduction of active power on the feeder and reactive power support of DGs, the all load nodal voltage along the feeder are increasing with different degrees. Thereby it enhances the carrying capacity of distribution network. However, if the location of the DG is on the power grid node of the substation, it can only enhance the total capacity of the substation, but cannot improve the load bearing capacity of the distribution line. Therefore, the influence of

the DG on distribution network is closely related to their location and capacity.

In addition, the interface types between the DG and distribution network are various, such as power electronic converters, synchronous generators, asynchronous generators groups, etc. Different types of interface with the power grid have different impact on the voltage stability of distribution network.

At present, the indexes measuring the voltage stability are sensitivity index, singular value index, margin index, L indicators, etc. Among them, the load margin index has been widely used because it can better quantify the distance from the current system running point to voltage collapsed point [23]. The key of load margin index calculation is to determine the voltage stability limit point. The specific methods include single-power-single-load node method, the multi-solution flow method, the nonlinear programming method, load admittance method, continuous flow method, etc. The Continuation Power Flow (CPF) method can not only effectively overcome the singular problem of Jacobi matrix near the saddle-node bifurcation point, but also track the power flow solutions under different load models. Its positive adaptability to the models makes it an important tool for analysis of the power system safety and voltage collapsing.

The CPF method along the PV curve searches the voltage stability limit point step by step, including four parts: prediction, parameterization, calibration and step control. It calculates many power flow solutions, with the large amount of computing and time. The way to improve the efficiency of continuous flow method is to choose a reasonable step control strategy. The larger step size would increase the number of iterations, even divergence, but too small step size will increase the computing time. The choice of step size control strategy also depends on the other three parts. This paper has improved the continuation flow method by using quadratic interpolation polynomial to estimate the voltage stability limit point and to obtain the next power flow solution, and adopting the self-adaptive step-change control strategy to accelerate the calculating of voltage stability limit point.

Basic continuation power flow equation can be expressed as:

$$H(X,\lambda) = f(X) + \lambda b = 0 \tag{6}$$

where X is the system state variable, $f(X) = 0$ is the conventional power flow equation, corresponding to the power flow solution when the initial state $\lambda = 0$, b denotes the grow direction vector of the load and generator, λ is grow coefficient. The common solution method for solving this equation is the predictor-corrector method. Traditional forecasting method is tangent or secant method, which are both linear. In order to reduce the number of iterations, it is often using small step forecast. Taking into account the Quasi Quadratic of λ–V or P–V curve, we can take advantage of the quadratic polynomial interpolation theorem, self-adaptive to change the step size according to the shape of the curve, and then find estimated value of the next point using polynomial extrapolation method. We can find the effect will be significantly improved.

Given that the quadratic interpolation polynomial of the ith PQ node is:

$$\lambda_i = a_i V_i^2 + b_i V_i + c_i \tag{7}$$

where a_i, b_i, c_i are the undetermined coefficients.

According to the interpolation theorem, the equation can be uniquely determined under knowing coordination of three points. For the first three points, according to the initial conditions of the system, a power flow solution A can be obtained; when given the load growing direction, choosing the smaller fixed load step size $\Delta\lambda$, the second and third flow solutions are obtained by using the tangent method and the secant method to estimate and by using continuation power flow to calibrate. When the three flow solutions are obtained, they are assumed to be A (V_{iA},λ_{iA}), B (V_{iB},λ_{iB}), C (V_{iC},λ_{iC}), shown in Fig. 2:

$$a_i = \frac{\frac{\lambda_{iC}-\lambda_{iB}}{(V_{iC}-V_{iB})} - \frac{\lambda_{iB}-\lambda_{iA}}{(V_{iB}-V_{iA})}}{(V_{iC}-V_{iA})} \tag{8}$$

$$b_i = \frac{\lambda_{iB}-\lambda_{iA}}{V_{iB}-V_{iA}} - a_i(V_{iB}+V_{iA}) \tag{9}$$

$$c_i = \lambda_{iA} - b_i V_{iA} - a_i V_{iA}^2 \tag{10}$$

Therefore the extreme point of the quadratic curve can be estimated, corresponding to the voltage stability limit point in Fig. 2, namely D ($Vicr$,$\lambda imax$).

$$V_{icr} = -\frac{b_i}{2a_i} \quad \lambda_{\mathrm{imax}} = c_i - \frac{b_i^2}{4a_i} \tag{11}$$

However, it is not appropriate to estimate the static stability limit point only by the first three power flow solutions. The power flow equation only can be expressed as a quadratic polynomial at the limit point, so the limit point estimated is far from the actual point, which need constantly update these three points by the appropriate step size control, and need repeat quadratic interpolation, to make them as close as possible to the extreme point, and then the static stability limit point calculated would be more precise.

In order to make computing faster to reach the limit point without affecting the accuracy of the solution curve, the paper using Eqn. (12) to predict the next iteration step.

$$\lambda^{(i+1)} = \alpha\lambda_{\max} + (1-\alpha)\lambda^{(i)} (0 < \alpha < 1) \tag{12}$$

where α is the step factor, usually taken to be 0.5, $\lambda_{\max}$ is the slope of the key nodes or nodes with the fastest voltage drop.

The change of λ, $\Delta\lambda$, *is* getting smaller and smaller when node is close to the stability limit point. Ideally, at the extreme point $\Delta\lambda_{cr} = 0$. In order to ensure a stable numerical solution of power flow equations, the article uses the static voltage stability sensitivity criterion [12] to test if the solution curve reaches the extreme point:

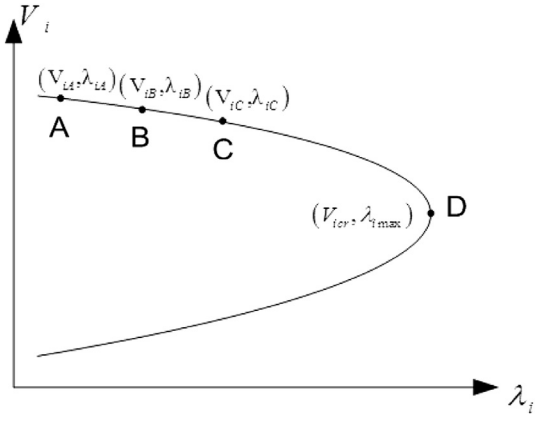

Fig. 2. Predict λ–V curve in interpolation polynomial.

$$\left|\frac{d\lambda}{dV}\right| = |2aV + b| < \beta \tag{13}$$

where a, b are the parameters of nodes with the fastest voltage drop in Eqn. (7), V is the voltage value of the node in the current power flow solution. The smaller the value of β is, the more close to the extreme point the flow solution is.

2.3. The choice of DG capacity and location on the power grid

The important subject of the DG at planning stage is the selection of the DG capacity and the location on the power grid.

Studies have shown that the DG's different installation location and capacity will affect the amplitude of the system short circuit current, voltage stability, voltage across in the distribution network, etc. The reasonable installation location can effectively improve the voltage stability of distribution network and the power factor of the system load, reducing the system active power loss. On the contrary, if not configured properly, it may have opposite effect on the power grid safety and stability [23]. In this paper, some simulation results and discussions are given below.

2.4. Simulation results

Based on the IEEE 30-bus standard system, the paper analyzes the static voltage stability limit of the power grid with the DG. The structure of the system is shown in Fig. 3.

Firstly, we can code voltage stability limit calculation program of IEEE 30-bus standard system in Matlab using the improved continuation power flow method mentioned above, and then draw the upper half branch of the PV curve according to the first five nodes with the fastest voltage drop, as shown in Fig. 4.

According to the P–V curve shown in Fig. 4, when the voltage is growing proportionately by the load constant power factor, the voltage drop of No. 30 node is the fastest, $\lambda_{max} = 2.957961$.

Shown in the system structure, in the first five nodes with the fastest voltage drop, 26, 29 and 30 nodes are all with load. In order to improve the utilization of DGs and strengthen the support to the power grid, DGs are installed in the load nodes with the lowest voltage. It is assumed that the power factor of DG is 0.9, the apparent power is the integer multiple of 0.1 MVA and not greater

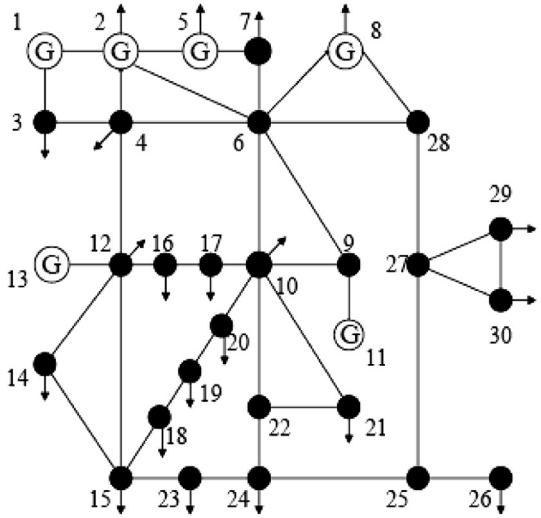

Fig. 3. Structure of IEEE 30-bus system.

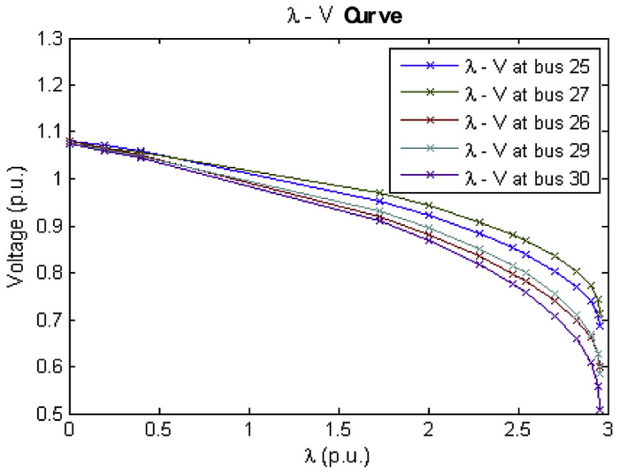

Fig. 4. λ–V curves of buses without DG.

than the load of the node, namely, $P_{DG} < P_L$. The total installed capacity of DG shall not exceed 10% of the total maximum load.

In this example, wind power generation is connected on the 30th bus, network capacity is 5 MVA, and the power factor is 0.98 based upon constant power factor proportional growth of load. The PV curve of the power grid with the DGs as shown in Fig. 5, the stability limit of the system is $\lambda_{max} = 3.394570$, higher than the original system by 14.7%, while No.26 node becomes the weakest node of system, and the voltage stability of No. 30 node has increased, indicating that the DG on No. 30 node will help improve the stability of this system.

3. The transient effect of DG and load on the power grid

3.1. Transient impact of DG under islanding operation

Fig. 6 is the microgrid simulation model. This microgrid contains 5 distributed generations, and 4 load models as follows: Load1 and classical synthesis load connected to the bus D_Grid, Load2 connected to the bus L1_PQ, Load3 connected to the bus L2_Vf. In islanding operation, DGs in the microgrid supply power for load together; in parallel operation, microgrid via a transformer connected to 10 kV power distribution network. The storage battery

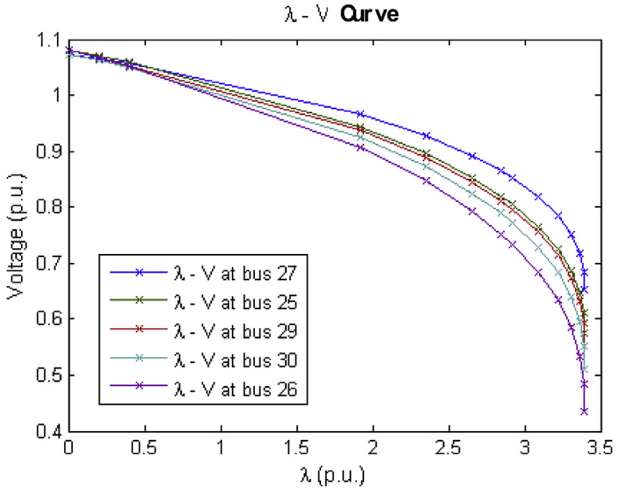

Fig. 5. λ–V curves of buses with DG.

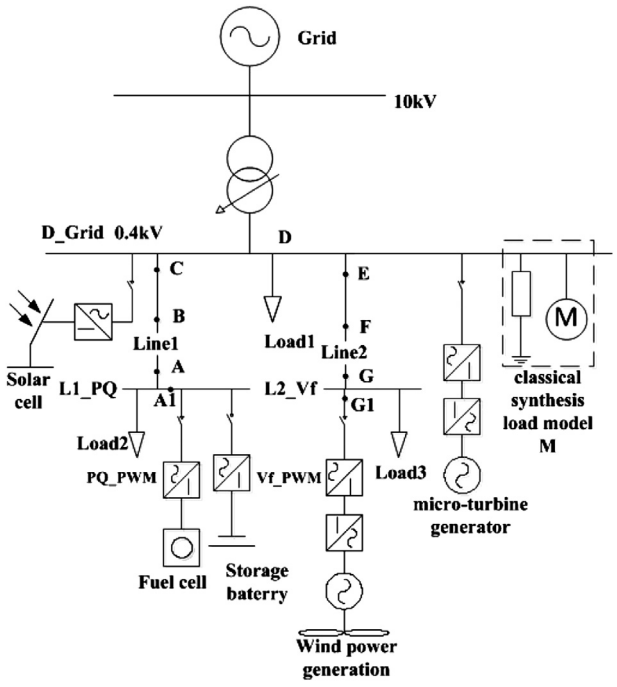

Fig. 6. Microgrid simulation model.

under PQ control connects to bus L1_PQ, and the Wind power generation under V/f control connects to bus L2_Vf.

Line1 and Line2 use cable-line model of software PSCAD. Load1, Load2 and Load3 are constant power load; Specific parameters of simulation model are shown in Table 1. The head of Line1 is connected to bus L1_PQ, and the head of Line2 is connected to bus L2_Vf, where A, B, C, D, E, F, G are the different three-phase short circuit fault location as shown in Table 2. Taking the most serious fault, namely, three-phase short circuit fault as an example, the output characteristics of DG with different inverter control mode would be analyzed.

Fig. 7 is the output (G1) characteristics of DG, namely wind power generation with V/f control. The inverter of Vf_PWM adopts constant voltage and frequency control. From the Fig. 7 we can see that, the closer fault point to the DG, the smaller equivalent impedance of system is, the greater output current is, and the greater output power is. When the output power limit is reached, the Vf_PWM, as microgrid energy balance regulator, will not be able to continue to maintain the constant voltage control, then the outlet voltage is dropping, the smaller the output voltage is, the greater the current is.

Fig. 8 is the output (A1) characteristics of DG, namely fuel cell, under PQ control. The PQ control is different from the V/f control, because its purpose is to make constant active power and reactive power output of DG, it cannot maintain the system's voltage and frequency. So in island operation, DG of constant power control

Table 1
Parameters of simulation model.

Short circuit capacity of system	Microgrid voltage (point D)	
31.4918 MVA	0.4 kV	
Load1 capacity	Load2 capacity	Load3 capacity
0.1 MW, 0.1MVar	0.1 MW, 0.05MVar	0.1 MW, 0.05MVar
Capacity of inverter Vf_PWM	Capacity of inverter PQ_PWM	
1.0 MVA	0.4 MVA	

Table 2
Fault location.

Fault point	The distance to bus L1_PQ
A	10% of Line1
B	50% of Line1
C	90% of Line1
D	100% of Line1
	The distance to bus L2_Vf
E	10% of Line2
F	50% of Line2
G	90% of Line2

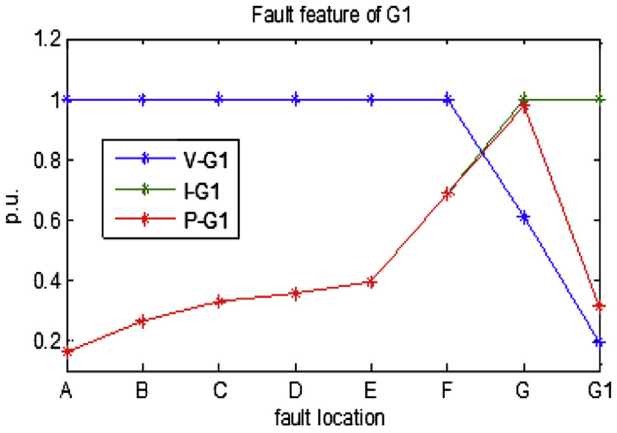

Fig. 7. Fault output characteristics of G1.

cannot supply power for load alone, needing to be matched with DG of V/f control.

The inverter PQ_PWM adopts constant power control. Fig. 8 shows, with the fault point from far to near, fault current is increasing, and fault voltage is decreasing correspondingly. When the PQ_PWM output current limit is reached, such as fault occurring at A, the DG is unable to maintain a constant output power, then the output power drops considerably, and fault current after reaching its limit, 2 times rated current, will no longer increasing.

Other output properties of DGs are similar with above.

3.2. Transient effect of motor load start on power grid

Ignoring the excitation reactance *Xm*, the current and electromagnetic torque equation of the rotor side are:

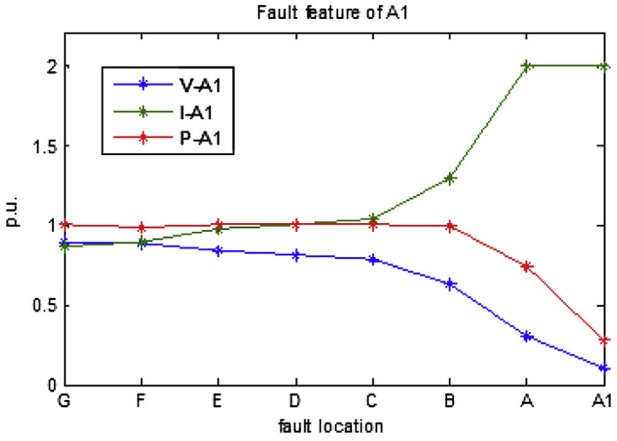

Fig. 8. Fault output characteristics of A1.

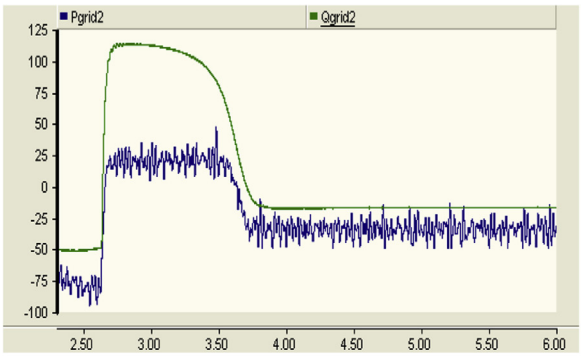

(a) The power curve of PCC point(kW, kVAR)

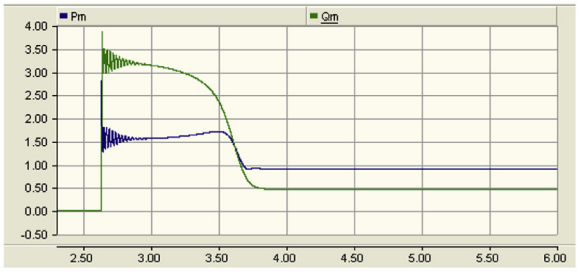

(b) The power curve of the induction motor(p.u)

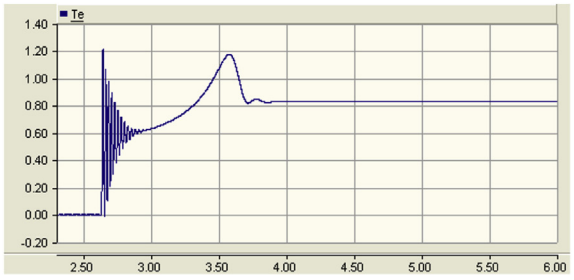

(c) electromagnetic torque of induction motor(p.u)

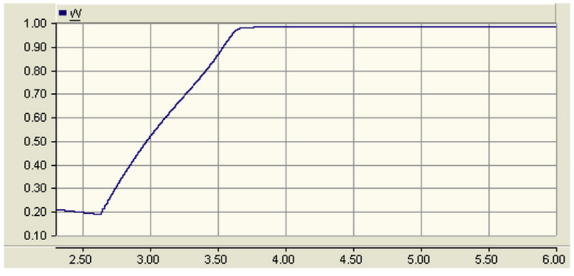

(d) speed of induction motor(p.u)

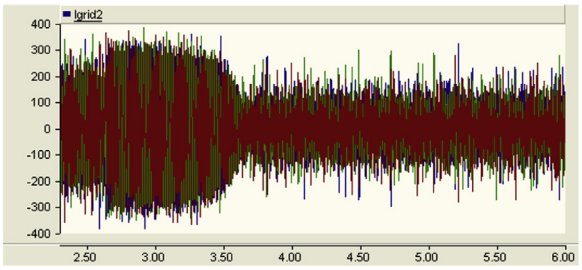

(e) Current at PCC point(A)

Fig. 9. Simulation of induction motor start.

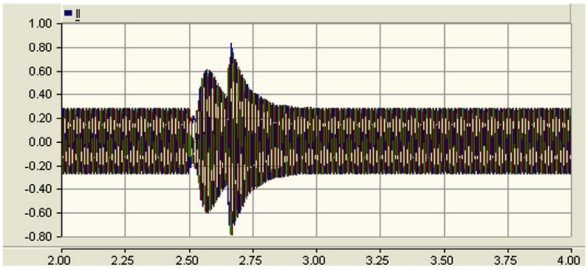

(a) the current of induction motor(A)

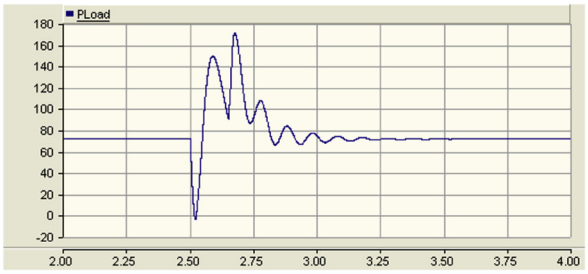

(b) active power of load with induction motor(kW)

(c) reactive power of load with induction motor(kVAR)

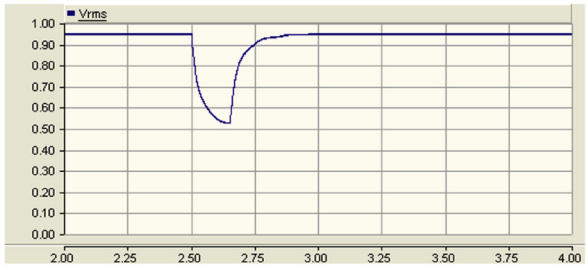

(d) Branch voltage of load with induction motor(p.u)

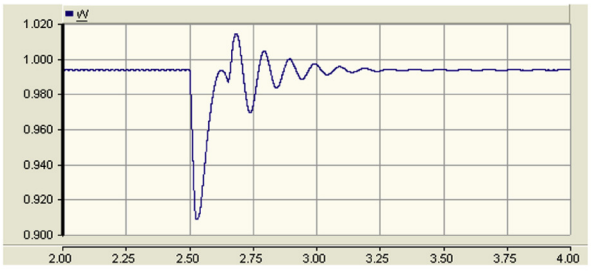

(e) Speed of the induction motor(p.u)

Fig. 10. Simulation of failures mode including the induction motor.

$$I_r = \frac{Vs}{(R_s + R_r/s) + (X_s + X_r)} \tag{14}$$

$$T_e = \frac{V_s^2 R_r}{(R_s + R_r/s)^2 + (X_s + X_r)^2} \frac{1}{s} \tag{15}$$

When the induction motor is starting, the rotor speed (n) is equal to 0 and the slip (s) is equal to 1. According to the Eqn. (14), the motor start current is very large, so that the stator and rotor leakage reactance will absorb a large amount of reactive power. When the DG uses the droop control, it contributes to the start-up protection of the motor, because when the power grid controllers of DG monitor the reactive power increasing, it will reduce the voltage so as to reducing the start current. On the contrary, the DG using V/f control will provide a larger current for the load to maintain constant voltage, which is not conducive to the over-current impact of grid-connected inverter. The DG using PQ control can generate the constant reactive power which has no impact on the starting process of motor load.

The paper analyzes the effect on the microgrid after induction motor starting. The simulation results are shown in Fig. 9 that the effect of induction motor on the microgrid cannot be ignored; it will produce a great starting current in the boot process and absorb large reactive power. The flow sent from the PCC point would be reversed. So it may cause the relay protection to malfunction in the microgrid.

We can see from Fig. 9(a) that the microgrid originally provides reactive and active power to the distribution network. When the induction motor is being started up, it will absorb a large amount of reactive power, so that the original power flow is reversed, and current at PCC point increases. When the motor is stable, the power input to distribution system is restored. In addition to maintain the stable operation of the motor, the microgrid can still transport a small amount of remaining power to distribution system, but the volume has been reduced. Thus DGs in the microgrid can maintain their isolated operation after the system is powered down, so as to ensuring the reliability of power supply within the microgrid.

3.3. Transient effect on load branch after fault

The section analyzes the effect on the motor load model, when there is a fault on the other branch of grid. Assumed that the main network three-phase short circuit occurs at $t = 2.5$ s, the fault is eliminated after 0.15 s. The voltage and current of load model with the induction motor shown in Fig. 10.

Shown in Fig. 10, when the fault occurs, the voltage and speed would drop down and current flowing into the induction motor load would increase, and the demand reactive power decreases rapidly; when the fault disappears, the voltage and the speed increase, as well as the current and reactive power, which is the same situation as the start process of induction motor.

4. Conclusions

In the paper, the static stability effect of DGs on the power grid has been studied firstly. In IEEE 30-bus system, an improved continuation power flow method is used to obtain voltage stability limit of power grid with or without DGs, respectively. This paper also analyzes the impact of DGs to load margin, which would contribute to the voltage stability of distribution network in the city.

Then, through the PSCAD software simulating the transient model the microgrid, this paper makes the output characteristics simulation of DG with different control strategies under different fault point. Compared with parallel operation, the limit of output fault current is small under island condition, because of the limit of DG short circuit capacity and current limiting link of inverter. Due to the special fault output characteristics of DGs, it will lead that the traditional distribution network protection cannot meet the requirements.

At last, it discusses the dynamic impact of the motor start-up and power grid fault on the microgrid. This paper analyzes the effect of composite load model, including DGs and induction motors. Simulation results show that induction motor model is very important to the study of microgrid system. To sum up, the modeling of microgird under island operation and loads with DGs would help in-depth study of the microgrid stability and the protection design of distributed network with DGs in the future.

Acknowledgments

Project Supported by National Natural Science Foundation of China (51077092) and 863 project (2011AA5A108)

References

[1] Zhanghua Zheng, Qian Ai. Present situation of research on microgrid and its application prospects in China. Power System Technology 2008;32(16):27–31.
[2] Junhong Wu, Qian Ai. Approach to improve power quality in distributed generation system. Low Voltage Apparatus 2009;12:45–9.
[3] Ting Lei. Strategy and coordinate control of distributed generation. Shanghai Jiaotong University; 2011.
[4] Lin Yu feng, Zhong Jin. Converter controller design methods for wind turbine systems in the DC micro grid [C]. In: Power and energy society general meeting–conversion and delivery of electrical energy in the 21st century. Pittsburgh: IEEE; 2008. p. 1–6.
[5] Xingyuan Li, Xiuying Wang. Fast voltage stability analysis methods based on static equivalence and singular value resolution. Proceedings of the CSEE 2003;23(4):1–5.
[6] Xiong Pan, Guoyu Xu. OPF based ATC calculation with static voltage stability constraints. Proceedings of the CSEE 2004;24(12):86–91.
[7] Jinquan Zhao, Xiaodong Jiang, Boming Zhang. An on-line enhancement control algorithm for static stability in power system. Proceedings of the CSEE 2005;25(8):7–12.
[8] Xiaoyan Qiu, Xingyuan Li, Wei Lin. Method for contingency screening and ranking for on-line voltage stability assessment. Proceedings of the CSEE 2004;24(9):50–5.
[9] Qian Ai. Power system identification by intelligent methods [M]. Shanghai Jiaotong University Press; 2012.
[10] Xianzhong Duan, Yangzan He, Deshu Chen. On some practical criteria and security indices for voltage stability in electric power system. Automation of Electric Power Systems 1994;18(9):36–41.
[11] Kundur Prabha. Power system stability and control [M]. McGraw-Hill, Companies; 1994. p. 1–39.
[12] Carson WT. Power system voltage stability. New York: McGraw-Hill; 1994.
[13] Long B, Ajjarapu V. The sparse formulation of ISPS and application to voltage stability margin sensitivity and estimation. IEEE Transactions on Power Systems 1999;14(3):944–57.
[14] Ruipeng Guo, Zhenxiang Han. An improved zeroeigen value method for point of collapse. Proceedings of the CSEE 2000;20(5):63–6.
[15] Li Xingyuan, Song Yonghua, Liu Junyong, Fu Ying, Zeng Min. Post-fault voltage security assessment of complex power systems based on ANN. Proceedings of the CSEE 1996;16(3):147–50.
[16] Yibo Wang, Chunsheng Wu, Hua Liao, Honghua Xu. Steady-state power flow analyses of large-scale grid-connected photovoltaic generation system. Journal of Tsinghua University (Science and Technology). 2009;49(8):1093–7.
[17] Hai-yan Chen, Jin-fu Chen, Xian-zhong Duan. Study on power flow calculation of distribution system with DGs. Automation of Electric Power Systems 2006;30(1):35–40.
[18] Wei Li, Yong Yang. Distribution network power flow algorithm of distributed power supply. Agriculture Network Information 2010;2:127–9.
[19] Changgui Wang, Sicheng Wang. Solar power generation practical techniques. Chemical Industry Press; 2005. p. 8–17.
[20] Yun Tiam Tan, Kirschen DS. Impact on the power system of a large penetration of photovoltaic generation [C]. IEEE power Engineering Society general meeting. Tampa, USA; 2007. p. 1–8.
[21] Zheng-ming Zhao, Jianzheng Liu, Xiaoying Sun. The solar power generation and its application. Science Press; 2005.
[22] Tao Yu, Jia-peng Tong. Modeling and simulation of the micro turbine generation system. Power System Protection and Control 2009;37(3):27–31. 45.
[23] Tingting Zhang. Study on siting and sizing of DG in distributed network planning. Southwest Jiaotong University; 2010.